Plasma Sources Sci. Technol. **18** (2009) 035002 (11pp) doi:10.1088/0963-0252/18/3/035002

Equilibrium states of anodic double layers

S D Baalrud, B Longmier and N Hershkowitz

Department of Engineering Physics, University of Wisconsin-Madison, 1500 Engineering Drive, Madison, WI 53706, USA

E-mail: sdbaalrud@wisc.edu

Received 14 January 2009, in final form 25 March 2009
Published 28 April 2009
Online at stacks.iop.org/PSST/18/035002

Abstract

Equilibrium states of anodic double layers that form near a positively biased disk-shaped electrode immersed in a partially ionized plasma are studied experimentally using electrostatic probes. When the potential drop from the electrode to the plasma is less than a critical value, $\Delta\phi_c$, an anode glow is observed where a double layer potential drop is within a few millimeters of the electrode surface. For larger biases an anode spot forms where the double layer potential drop is centimeters from the electrode and the intervening region is a plasma more luminous than the bulk plasma. A theoretical model is developed which predicts that $\Delta\phi_c \propto 1/P + C$, where P is the neutral pressure and C is a constant, and it predicts hysteresis in the current–voltage characteristic at the electrode; both effects are observed experimentally. The model also provides an estimate for the distance between the electrode and double layer potential drop that agrees with the measurements. Near small electrodes, anode spots are observed to be 'fireballs,' which are spherical in shape. Near larger electrodes 'firerods' are found instead, which have a cylindrical shape. It is shown that firerods are required by global current balance because they have a smaller effective electron collecting area than fireballs. Experiments also confirm that global nonambipolar flow (Baalrud S D *et al* 2007 *Phys. Plasmas* **14** 042109) accompanies firerods. In this case all electrons are lost through the firerod to the electrode, while all positive ions are lost to the other plasma boundaries.

(Some figures in this article are in colour only in the electronic version)

1. Introduction

Anodic double layers, among the many discoveries of Langmuir [1], are adjacent regions of positive and negative space charge that can form near plasma boundaries biased more positive than the plasma potential. Typically, the potential profile near positive boundaries, e.g. electrostatic probes, monotonically decreases with positive curvature to the plasma potential with an exponential behavior and on a length scale characteristic of the Debye length. The term 'electron sheath' is often used to describe this situation because the thin region with electric field contains mostly electrons. Anodic double layers, on the other hand, have potential profiles with both positive and negative curvature. Their potential profiles can be monotonically decreasing, but need not be, and they can occupy spaces near the anode ranging from Debye length scales to much longer length scales characteristic of a presheath.

Anodic double layers can form from a variety of different physical mechanisms, and should be classified accordingly. One mechanism is increased ionization from electrons energized by the electron sheath electric field. This leads to the two types of anodic double layers photographed in figure 1: thin 'anode glows' and much thicker 'anode spots.' As the electrode bias is increased, starting from some low level, the anode glow forms at a value for which the electron energy gained in the electron sheath exceeds the electron-impact ionization energy of the neutral gas. Ions are then born in the sheath with energy characteristic of the thermal energy of the neutral gas. They are pushed into the plasma by the electron sheath electric field at a rate much slower, by a factor of the square root of electron to ion mass ratio $\sqrt{m_e/M_i}$, than the electrons are pulled to the electrode surface. A thin region of net positive space charge near the electrode, i.e. an anodic double layer, can thus form. At some even larger positive electrode bias, the thin anode glow rapidly transitions to a much thicker anode spot. In this paper we test the hypothesis that this transition occurs when the number of ions in a Debye cube on the high potential side of the double layer approximately balances the number of electrons in the same Debye cube; thus establishing a quasineutral region.

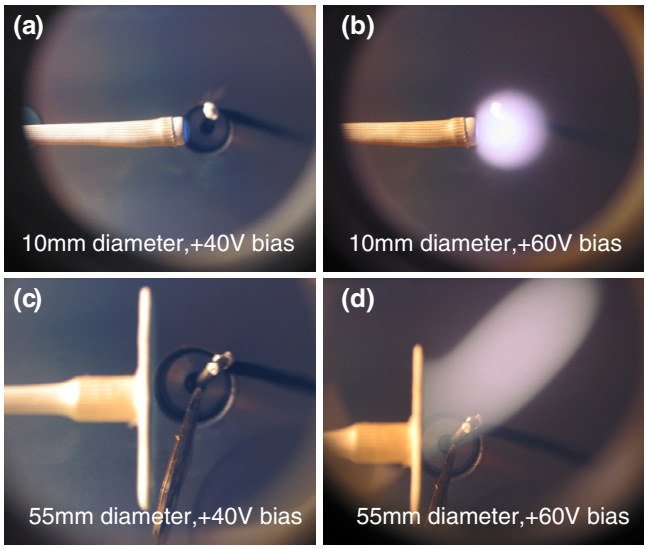

Figure 1. Photographs of equilibrium states of anodic double layers. Anode glows: (*a*) near a 1 cm diameter electrode and (*c*) near a 5.5 cm diameter electrode. Anode spots: (*b*) shows a fireball and (*d*) a firerod. The background shows an ion acoustic wave launcher and its holder that were not used in this experiment.

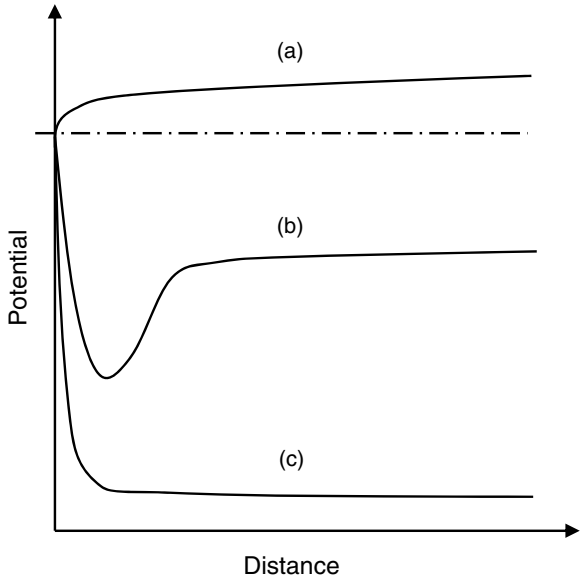

Figure 2. Sheath solutions for an electrode biased more positive than other plasma boundaries include (*a*) an ion sheath, (*b*) a double sheath and (*c*) an electron sheath.

Other types of anodic double layers can also form, e.g. double sheaths, where increased ionization does not occur. Double sheaths consist of an electron sheath adjacent to a double layer and do not have monotonically decreasing potential profiles. Their potential profile typically appears to contain a 'dip' in an otherwise monotonic electron sheath. See, for example, the data presented in figure 2 of [2], or the schematic drawing in figure 2(*b*). Double sheaths can form in several circumstances including the presence of ion beams [3], applied magnetic fields [4], or as a result of non-local effects such as global balance of electron and ion currents lost from a plasma [2]. In this paper we report that double sheaths and anode spots can sometimes be present in combination as well.

Anode glows and spots have previously been studied by several researchers. They have been mentioned in double layer reviews recently by Charles [5] and in 1982 by Emeleus [6]. The transition from electron sheath to anode glow has been observed experimentally [6] and was numerically investigated by Conde *et al* [7]. Anode spots have been observed to have a spherical shape, first called 'fireballs' by Song *et al* [8], and subsequently by others [9–15], or a cylindrical shape, first called 'firerods' by An *et al* [16], and subsequently by others [17, 18]. Multiple fireballs have also been observed either as nested concentric spheres, 'multiple concentric double layers,' [19–26], or at multiple distinct locations on the anode surface, 'non concentric multiple double layers' [20, 21, 23, 27, 28].

Anode spots have been studied in both unmagnetized plasmas [8, 12, 13, 28–31], and in magnetized plasmas [13, 32–34]. Their stability has been investigated in detail experimentally [8, 29, 35] and theoretically [9, 12, 36–38]. Recent work of Stenzel *et al* [13] details the dynamics of anode spot formation. Anode spots have also been used to confine dust particles [17]. Among the properties of anode spot equilibrium reported are the observation that hysteresis accompanies the onset of an anode spot as measured from a current–voltage characteristic on the electrode where the electrode bias must be greater for onset of the anode spot than is required to maintain it [8, 10, 11, 15]. The critical electrode bias necessary for the onset of the anode spot and its characteristic dimension are inversely proportional to the neutral pressure [8]. Also, the potential profile and location of the DL potential drop in relation to the electrode was investigated for fireballs [8, 23]. Firerods have until recently only been reported in magnetized plasmas [16–18]. However, Stenzel [13] reports their observation in unmagnetized plasma near a spherical electrode. Here we report the observation of firerods near disk-shaped electrodes in unmagnetized plasma.

In this paper we address three questions related to anodic double layer equilibrium: (1) What causes the transition from uniform anode glow to anode spot? (2) Why is this transition accompanied by hysteresis? (3) In an unmagnetized plasma, why is the anode spot sometimes spherical, a 'fireball,' and sometimes cylindrical, a 'firerod'. We also show that the presence of an anode spot can cause global nonambiplolar flow where all electron loss from the plasma is through the anode spot to the electrode, while all positive ions are lost only to the cathode, which is the grounded chamber wall in our experiments [2]. The anode spot geometry is also related to these global characteristics.

This paper is organized as follows. In section 2 we describe the experimental apparatus and diagnostics. The important experimental results follow in section 3. Section 4 details anode glow equilibrium and the conditions required for it to exist. In section 5 we present a model for the transition from anode glow to anode spot modes. The model predicts hysteresis in the current–voltage characteristic and an inverse neutral pressure dependence for the anode bias required for anode spot onset. In section 6 we show that small electrodes can support spherical anode spots, i.e. fireballs, but that larger

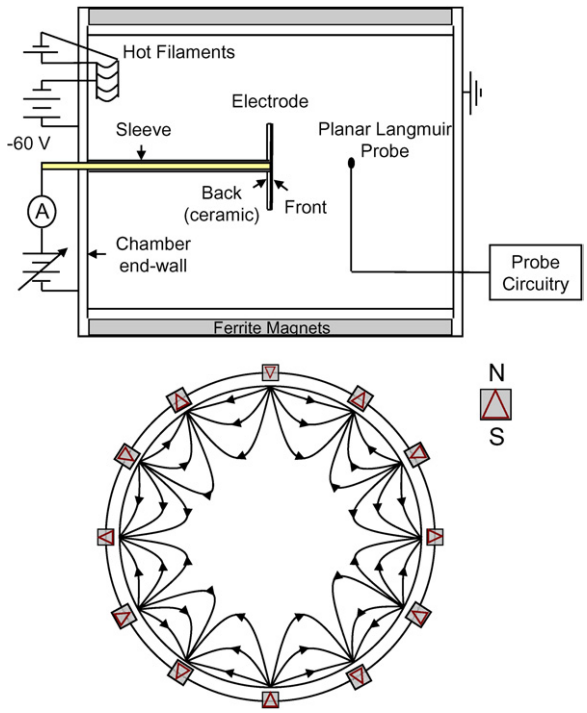

Figure 3. Dc anodic double layers and sheaths were generated in front of a one-sided disk electrode submersed in a filament generated argon plasma in a MacKenzie bucket.

electrodes typically host cylindrically shaped anode spots, i.e. firerods. Experimental data show double sheaths on an electrode with a firerod at locations where the firerod was absent. A model for these effects, which is based on global current balance, is developed and compared with data. It is shown that global nonambipolar flow happens when firerods are present. Implications for multiple concentric double layers are briefly discussed.

2. Experimental apparatus and diagnostics

Experiments were conducted in a cylindrical MacKenzie bucket [39] 70 cm in length and 60 cm in diameter, see figure 3. Twelve rows of permanent ferrite magnets of alternating polarity surrounded the cylindrical wall of the chamber to create a uniform discharge in the radial direction. The peak field near the cylindrical walls was approximately 1 kG, while the field on axis was less than 2 G. Due to the low magnetic fields in the bulk plasma the experimental region was essentially not magnetized. No magnets were placed near the chamber end walls.

Plasmas were created from ionization of argon gas by emission of a 0.5 A electron current by heated thoriated tungsten filaments near one chamber end wall. The filaments were biased at −60 V (all electric potentials are referenced to the grounded wall of the vacuum chamber). Base vacuum pressure was less than 1 μTorr and operating neutral pressures ranged from 0.5 to 5 mTorr.

Anodic double layers were created near aluminum electrodes held in the center of the vacuum chamber by a 0.6 cm diameter copper rod. The 'back' side of each electrode was electrically insulated from the plasma using ceramic insulator. The copper rod holding the electrodes was insulated from the plasma using a thin fiberglass sleeve. Electron sheaths and anodic double layers were observed near the 'front' electrode surface when the electrode was biased more positive than the plasma potential. The electrode area was varied by choosing electrodes of different radii.

Plasma potential, electron temperature and electron density were measured in the bulk plasma using an 8 mm diameter, disk-shaped, planar Langmuir probe. Measurements were taken on the chamber axis 15–20 cm from the 'front' electrode surface to ensure that the probe was in the bulk plasma rather than in the sheath, presheath or double layer surrounding the electrode. The plane of the Langmuir probe was oriented parallel to the plane of the electrode and its 8 mm diameter was much longer than the plasma Debye length, which was typically 0.1–1 mm. Typical plasma densities ranged from 1–5 $\times$ 10^9 cm^{-3}, and electron temperatures from 0.5 to 3 eV.

3. Experimental Results

Schematic drawings of electron sheath, anode glow, and anode spot potential profiles are shown in figure 4(*a*). For an electron sheath, the potential drops from the electrode potential to the plasma potential within a few Debye lengths. This distance extends to approximately 10 Debye lengths as an anode glow forms. Upon onset of an anode spot, the double layer potential drop relocates to hundreds of Debye lengths from the electrode, corresponding to the ion–neutral collision length scale, and the potential fall corresponds to the electron-impact-ionization energy of the neutral gas.

Emissive probe measurements of the potential profile for each of these solutions are shown in figure 4(*b*). These data were taken at 1 mTorr pressure with a 5.5 cm diameter electrode biased at 20 V for the electron sheath, 40 V for the anode glow, and 60 V for the anode spot. In this case the anode spot was a firerod, like that in the photograph shown in figure 1(*d*). An important feature of the data is that the anode glow was much thicker than the electron sheath. However, the sign reversal of the curvature of the potential profile, which is representative of a double layer, could not be resolved by the emissive probe diagnostic. As sketched in figure 4(*a*), the spatial extent of this region is a few Debye lengths. The Debye length was approximately 0.2 mm in this plasma, and the spatial resolution for the probe was approximately 1 mm. Figure 4(*b*) shows that the anode spot has a characteristic length of approximately 2 cm and a potential drop of approximately 17 V, which corresponds to the argon ionization potential.

The critical electrode bias for which the rapid transition from anode glow to anode spot occurs is shown to be inversely proportional to the neutral gas pressure within a constant. These data are shown in figure 5 for electrode diameters of 1 and 5.5 cm. Figure 5 also shows that the electrode diameter influences the critical electrode bias. Stenzel *et al* [13] provided a detailed study of the dynamics of this transition and showed that its characteristic timescale is 10–100 μs. In our data, the critical bias was determined for each data point by slowly increasing the electrode potential, starting at zero,

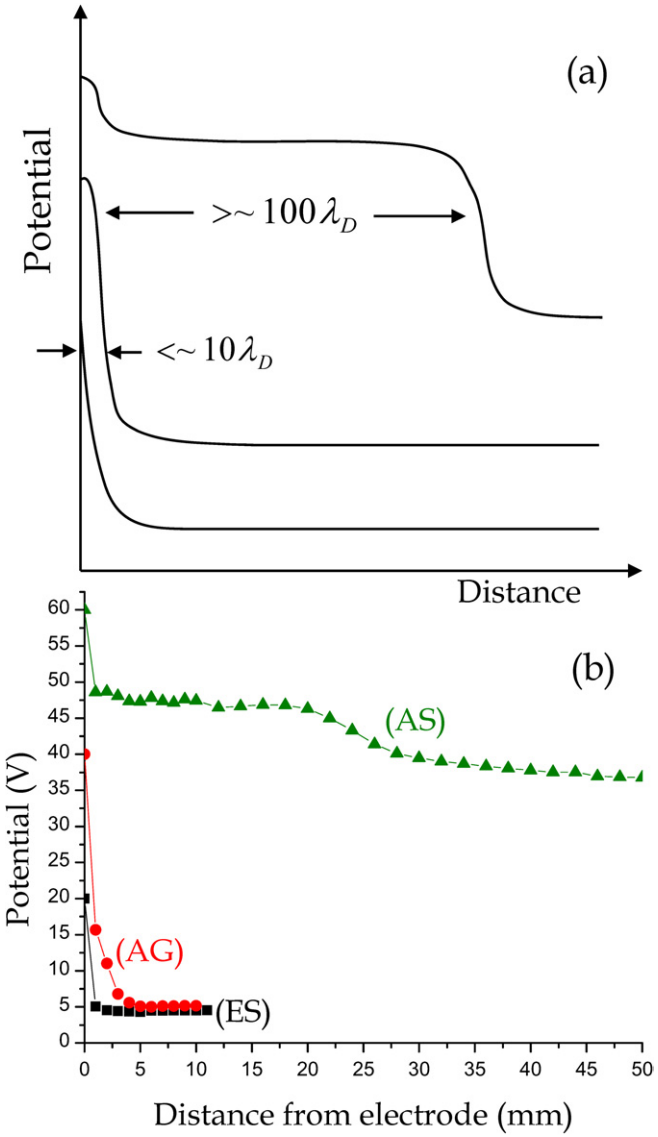

Figure 4. (*a*) Schematic drawing of anode spot (AS), anode glow (AG) and electron sheath (ES) potential profiles. (*b*) Emissive probe measurements of each solution for an electrode biased at 20V for the electron sheath, 40 V for the anode glow, and 60 V for the anode spot (which in this case was a firerod).

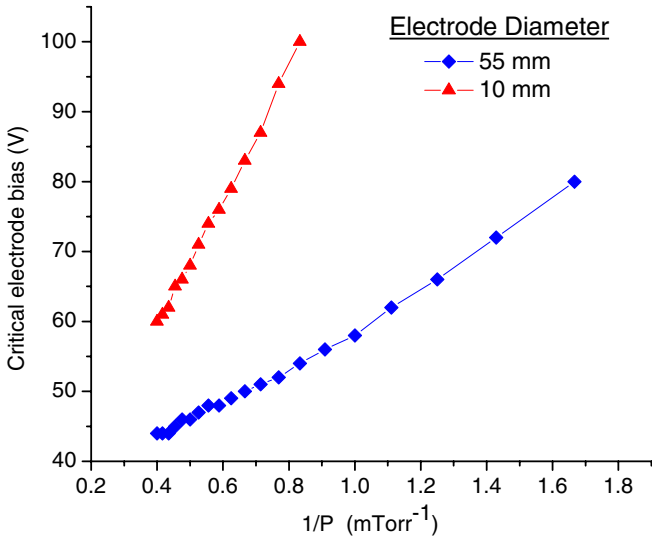

Figure 5. The critical electrode bias for onset of an anode spot is shown to be proportional to $1/P + C$. Data shown are for electrode diameters of 1 cm (triangles) and 5.5 cm (diamonds).

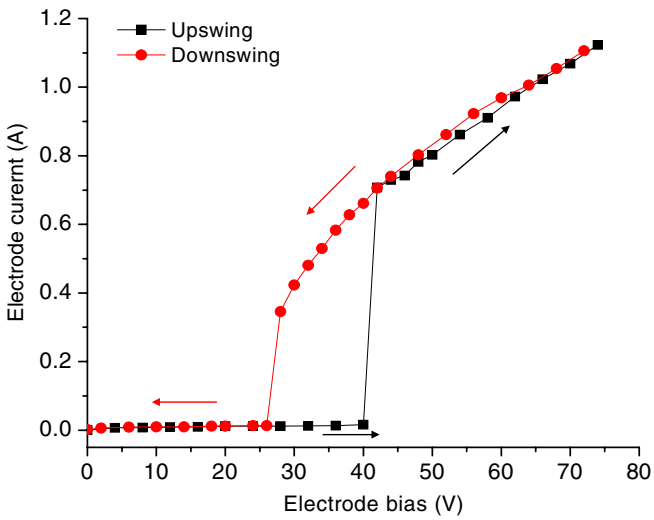

Figure 6. *I*–*V* characteristic for a 1 cm diameter electrode taken increasing the electrode bias (squares) and subsequently decreasing it (circles). The data show hysteresis in the bias required for anode spot formation and disappearance.

until the transition occurred. It is important to distinguish that the data were taken on the 'upswing' of the bias because after the anode spot has formed smaller electrode biases can still maintain it. This feature appears as hysteresis in the current–voltage characteristic of the electrode.

Figure 6 shows the current–voltage characteristic of a 1 cm diameter electrode. The current is shown to be much larger in the anode spot mode than the anode glow mode. This can be attributed to a relative increase in the effective area for electron collection to the electrode in the spot mode than the glow mode. Current due to electrons born by ionization inside the anode spot provides a much smaller, but finite, additional electron current as well. An important feature of this trace is hysteresis; the anode spot forms when the electrode is biased to 40 V, but then is maintained until the electrode falls below approximately 28 V.

Figures 7 and 8 show the behavior of bulk plasma potential and electron temperature for a similar trace of the electrode bias. In this case a 5.5 cm diameter electrode was used. These figures demonstrate two characteristic features of global nonambipolar flow when the anode spot is present: plasma potential 'locking' and an electron temperature increase [2]. Global nonambipolar flow occurs when the effective area for electron collection at the electrode is sufficiently large that it collects a total electron current that balances the total ion current lost to all the other boundaries of the plasma. In the case shown in figures 7 and 8 the formation of an anode spot causes such an increase in the effective electron collecting area. Figure 7 shows that the plasma potential locks to a value a few volts less than the electrode potential minus the ionization potential of the neutral gas. In previous work where anode spots were not present, but global nonambipolar flow

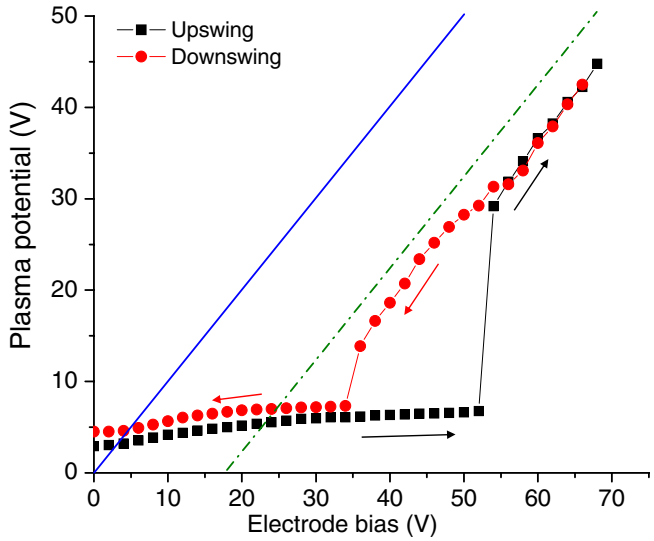

Figure 7. Plasma potential versus increasing (squares) and decreasing (circles) electrode bias. The solid line plots plasma potential equal to electrode bias, while the dash–dotted line shows the same less the ionization potential of argon.

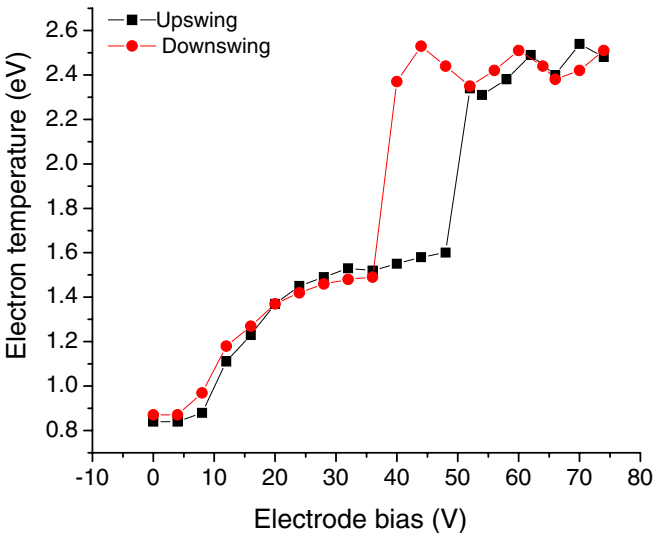

Figure 8. Langmuir probes measure a jump in the bulk electron temperature when an anode spot forms, which is indicative of global nonambipolar flow.

was achieved with larger electrodes, the locking potential was a few volts less than the electrode potential [2].

The shape of the spot, which in this case is cylindrical, is also related to the global flow scenario. Spots near small electrodes are typically spherical with a radius greater than the electrode diameter [3, 8, 10]. However, if such a spot were present near too large an electrode, the electrode would collect an electron current that exceeds the ion current lost to the other plasma boundaries. In this case the effective electron collecting area of the spot must shrink to preserve the balance of electron and ion currents lost from the plasma. The effective electron collecting area of an electrode typically shrinks by the formation of double sheaths which reflect a fraction of the incident electron current [2]. When anode spots were present, double sheaths formed on regions of the electrode surrounding the anode spot. In section 6 we present a one-dimensional model that suggests the length of the anode spot is fixed, so the radius of the spot is the only direction allowed to shrink. Thus, firerods form near large electrodes where large is defined by the effective electron collecting area of the electrode and spot. This prediction is in accordance with the observed geometries shown in figure 1 and double sheaths were measured on electrode locations near firerods. The effects of global nonambipolar flow on anode glow and spot equilibrium are discussed further in sections 4 and 6.

4. Anode glow

In order for an anodic double layer to form, the electrode must be biased positive relative to the plasma potential; for anode glow or spot formation, in particular, it must be at least an ionization potential of the neutral gas, E_i/e, more positive (for $T_e \ll E_i$, which is the only case considered here). It was shown in [2], for the same geometry as this experiment, that three different sheaths, apart from glows or spots, can form near the electrode: electron sheath, double sheath or ion sheath. These are depicted in figure 2. Which solution occurs is determined by balancing the positive ion and electron currents lost globally from the plasma. Global current balance can be written as $\sum_s I_s = 0$ where

$$I_s = q_s \sum_k \int \boldsymbol{j}_s \cdot \mathrm{d}\boldsymbol{A}_k \times \begin{cases} \exp\left(-\dfrac{e\Delta\phi_k}{T_e}\right) & \text{retarding} \\ 1 & \text{attracting,} \end{cases} \quad (1)$$

in which $\boldsymbol{j}_s(\boldsymbol{x}) = \int \mathrm{d}^3 v \boldsymbol{v} f_s(\boldsymbol{x}, \boldsymbol{v})$ is the current density of species s, f_s is the velocity distribution function of this species and $\Delta\phi_k$ is the potential drop of any current retarding electric fields near surface k. If the sheath (or double layer) at a particular surface k (with differential surface area $\mathrm{d}A_k$) does not reduce the current of species s reaching that surface, i.e. only attracting potentials are present for s, the exponential term is absent from equation (1). If the species distribution functions, details of the bounding surface geometry, and their relative electrical potentials are known, equation (1) determines the bulk plasma potential.

For the geometry described in section 2 and assuming Maxwellian ion and electron species, equation (1) reduces to an expression which predicts that the electrode sheath is an electron sheath if $A_E/A_w < \mu$, an ion sheath if $A_E/A_w > [(0.6/\mu) - 1]^{-1}$ and a double sheath if $\mu < A_E/A_w < [(0.6/\mu) - 1]^{-1}$, see [2]. Here $\mu \equiv \sqrt{2.3 m_e/M_i}$, where m_e is the electron mass, M_i is the positive ion mass, A_E is the electrode surface area and A_w is the effective area for ion loss at the chamber walls. These three solutions are depicted in figure 2 for a fixed electrode bias, but different electrode surface areas. Also shown in [2] is that only for the electron sheath can the electrode be biased much more positive than the plasma. When a double sheath exists, the plasma potential is always a just few volts less than the electrode potential. The plasma potential is always more positive than the electrode bias with an ion sheath solution. In order for an anode glow or spot to form in our geometry the electrode surface area must be small enough that it satisfies $A_E/A_w < \mu$. When this condition is

satisfied and $-e\Delta\phi/E_i > 1$ at the electrode, an anode glow may form.

The transition from electron sheath to anode glow is accompanied by a thin glowing region on the surface of the electrode, see figure 1. The anode glow double layer forms when the local ion density in a thin region adjacent to the electrode exceeds the local electron density. These thin double layer potential profiles were studied numerically by Conde *et al* [7] who confirmed that they are, in fact, due to increased ionization in the electron sheath. Electrons born from ionization are pulled toward the boundary by the electron sheath electric field much faster, at a rate $\propto\sqrt{M_i/m_e}$, than the heavier ions are pushed to the plasma. A local ion rich region is left behind.

In Conde's numerical simulations the ion rich region (where the potential profile has negative curvature) was calculated to be shorter than 10 Debye lengths [7]. As we previously mentioned, such a thin region could not be resolved in this experiment. Figure 4 does show, however, that the electron sheath potential rise moves further from the electrode when the anode glow is present. This, along with the visible glowing region, provides evidence that a thin double layer was present.

5. Anode spot onset

Anode spots are characterized by a thick (typically hundreds of Debye lengths) glowing region of quasineutral plasma separating a double layer potential fall (of approximately the ionization energy of the neutral gas) from the electrode. In previous works, this abrupt transition was conjectured to depend on a local ionization instability that significantly increases the local ionization rate [35, 37]. However, numerical simulations of Conde *et al* [7] showed that such an instability is not necessary to produce the level of ionization required for a thin double layer, i.e. anode glow, but their simulations did not capture the abrupt transition to anode spot. We conjecture that this is because the transition depends on physics of quasineutrality that were not included in previous models.

When the density of ions in the ion rich region of an anode glow grows to a level such that a Debye cube contains an approximately equal number of electrons and ions, quasineutrality is established and a plasma is formed. When this occurs, ions leaving the newly established plasma must have a fluid speed in excess of the local ion sound speed c_s in order to be lost through, what appears to these ions, as an ion sheath into the bulk plasma. This is Bohm's criterion for an ion sheath [40]. Since the acceleration region that forms to satisfy this criterion must itself be quasineutral, it must be much longer than the Debye length scale in order to support the necessary potential drop of approximately T_e/e. This acceleration region is a main characteristic of an anode spot, and it is analogous to a conventional ion presheath.

To develop a simple model of this physics, consider the balance of fluxes of electrons and ions born from ionization leaving a sample Debye cube in an anode glow near an electrode; $\Gamma_{i,g} = \Gamma_{e,g}$. Subscript g denotes the anode glow region. The ion flux is $\Gamma_{i,g} = n_{i,g}\bar{v}_{i,g}$ where $n_{i,g}$ is the density of ions born in the Debye cube, $\bar{v}_{i,g}$ is the average ion speed at the ion exit (plasma side) of the Debye cube. The electron flux born from ionization in a Debye cube in the anode glow is $\Gamma_{e,g} = \Gamma_{e,b}n_n\sigma\lambda_{D,g} = n_{e,g}\bar{v}_{e,g}$, where $\Gamma_{e,b}$ is the beam flux of electrons entering the Debye cube from the bulk plasma through the electron sheath, n_n is the neutral density, σ the electron–neutral impact ionization cross section, $n_{e,g}$ is the density of electrons born from ionization in the Debye cube and $\bar{v}_{e,g}$ is the average electron speed at the electron exit (electrode side) of the Debye cube. Equating fluxes yields

$$n_{i,g} = \frac{\Gamma_{e,b}n_n\sigma\lambda_{D,g}}{\bar{v}_{i,g}}. \tag{2}$$

For a Maxwellian electron distribution in the bulk plasma, the electron flux entering an electron sheath (or anode glow) is $\Gamma_{e,b} = n_{e,p}\bar{v}_e/4$ in which $n_{e,p}$ denotes the bulk plasma electron density and $\bar{v}_e = \sqrt{8T_e/\pi m_e}$ is the mean electron speed in one direction.

Assuming energy conservation in the thin Debye layer implies that $\bar{v}_{e,g}/\bar{v}_{i,g} \approx \sqrt{M_i/m_e}$. Thus, flux conservation $\Gamma_{e,g} = \Gamma_{i,g}$ shows that ions born from ionization are much more dense than the electrons born from ionization in the Debye cube: $n_{i,g}/n_{e,g} \approx \sqrt{M_i/m_e} \gg 1$. In the electron sheath portion of the anode glow, $n_{i,g} \ll n_e$, where $n_e = n_{e,b} + n_{e,g}$ is the total electron density. Since $n_{i,g} \gg n_{e,g}$, nearly all of the electrons are due to the beam entering from the bulk plasma. As quasineutrality is approached in the Debye cube, $n_{i,g} \approx n_e$, but $n_{i,g} \gg n_{e,g}$ still implies that $n_{e,g} \ll n_{e,b}$.

Our conjecture is that rapid transition to an anode spot occurs when the number of electrons and ions in the Debye cube approximately balance

$$\int_{\lambda_{D,g}} dV n_{e,g} \approx \int_{\lambda_{D,g}} dV n_{i,g} \equiv N \tag{3}$$

in which the integrals span a sample Debye cube adjacent the electrode, and N represents the critical number of ions or electrons in the Debye cube. Estimating N is quite difficult since it requires a local estimate of the electron density and Debye length throughout the anode glow. As ions build up, the potential profile in this region begins to flatten, as shown in [7]. As a lowest order approximation, we assume $N \approx n_{i,g}\lambda_{D,g}^3$. With this, equation (2) implies

$$\frac{\Gamma_{e,b}n_n\sigma\lambda_{D,g}^4}{\bar{v}_{i,g}} \approx N \tag{4}$$

at the bias required for anode spot formation.

Although the beam electrons are responsible for the increased ionization, only a small fraction of the electron beam ionizes neutrals; so the flux and energy of the beam are assumed to approximately be conserved. This implies $\Gamma_{e,b} \approx n_{e,b}\sqrt{2e\Delta\phi/m_e}$ which, from the continuity equation, is approximately constant throughout the electron sheath and anode glow ($n_{e,b} \propto \Delta\phi^{-1/2}$). Using this expression along with $\lambda_{D,g}^2 = \epsilon_o T_e/e^2 n_e$, and $n_e \approx n_{e,b}$, equation (4) can be written

$$\Delta\phi_c = \frac{N}{\alpha}\frac{1}{n_n}, \qquad \alpha \equiv \frac{\epsilon_o^2 T_e \sigma v_{Te}^2}{e^3 \bar{v}_{i,g}\Gamma_{e,b}} \tag{5}$$

in which $\Delta\phi_c$ is the critical electron sheath potential rise required for the rapid onset of an anode spot, and α is a constant for argon gas at the relevant sheath energies in this experiment. $v_{Te}^2 = 2T_e/m_e$ is the electron thermal velocity. In general the cross section σ is energy dependent, i.e. it depends on $\Delta\phi_c$, and thus so does α. However, in the range of relevant electron energies for this experiment (40–100 eV) σ is approximately constant [41]. For α and N constant, we find

$$\Delta\phi_c \propto \frac{1}{n_n} \propto \frac{1}{P} \tag{6}$$

in which P is the neutral gas pressure.

In general α is not constant for all electron energies. In particular, the electron-impact ionization cross section rapidly vanishes at a threshold potential which determines a minimum $\Delta\phi_c$. If this cross section can be modeled as approximately constant above the threshold E_i/e one should find the scaling $\Delta\phi_c \propto 1/P + C$, where $C \geqslant E_i/e$ represents a minimum $\Delta\phi_c$.

Figure 5 shows close experimental agreement with the inverse neutral pressure dependence of the critical electrode bias, $\Delta\phi_c$, required for an anode spot to form over an electron energy range in which σ is approximately constant. Data is shown for electrode diameters of 10 and 55 mm. Differences in the slope of the two lines are apparently due to N/α not being the same for each electrode. This is expected since the bulk plasma parameters, e.g. density and electron temperature, are different for each electrode radius. Although the bulk plasma parameters were not sensitive to neutral pressure over this range, different sized electrodes, when biased more positive than the plasma, caused different plasma parameters. This is because the electrode sets the bulk plasma potential which, from global current balance, is found to increase with electrode surface area [2]. Filament injected electrons gain energy $e(V_p - V_f)$, where $V_p - V_f$ is the potential difference of the bulk plasma and filament bias. Thus the energy of injected electrons also depends on the electrode size and one should expect that N/α is not necessarily the same for each electrode diameter. This notion is confirmed in figure 5

Ideally one would like to calculate N and α. However, N requires a local solution for electron or ion density and Debye length. In addition, α requires the average ion speed leaving the Debye cube $\bar{v}_{i,g}$. An accurate calculation requires solving Poisson's equation along with the coupled two-fluid equations accounting for ionization throughout the electron sheath and anode glow. Such a theoretical exercise is outside the scope of this mainly experimental work, but we seek to obtain a crude estimate of these parameters for the data displayed in figure 5. For the relevant electron energies in this experiment, $40 < e\Delta\phi_c < 100$ eV, $\sigma \approx 2.5 \times 10^{-16}$ cm^2 [41]. We assume that N is approximately the same as the number of particles in a Debye cube in the bulk of the plasma, $N \approx n_{e,p}\lambda_D^3$, and use the formula $n_n \approx 3.3 \times 10^{13} p$ in which n_n is in cm^{-3} and p is in mTorr. Finally, for the crudest approximation, we assume that the ions leave the Debye cube with a speed approximately the sound speed, c_s. This last assumption is not due to Bohm's criterion, but is only used as an order-of-magnitude level approximation.

The experimentally obtained slopes, S, in the equation $\Delta\phi_c = S/p$ in which p is in mTorr, are $S \approx 29$ for the 55 mm diameter electrode, and $S \approx 100$ for the 10 mm diameter electrode, see figure 5. S is measured in [V mTorr]. For the 55 mm diameter electrode the bulk plasma density was $n \approx 1.2 \times 10^9$ cm^{-3} and the electron temperature was $T_e \approx 1.7$ eV for biases close to anode spot onset. These values were $n \approx 2.1 \times 10^9$ cm^{-3} and $T_e \approx 1.0$ eV for the 10 mm diameter electrode. With these bulk plasma parameters and the aforementioned assumptions, equation (4) predicts $S \approx 14$ for the 55 mm diameter electrode and $S \approx 16$ for the 10 mm diameter electrode. The corresponding estimates for N are approximately 2×10^4 and 9×10^3 respectively. These estimates for S are significantly less than the experimental results, but within the order-of-magnitude level approximation for $\bar{v}_{ig}$, which was quite crude. In reality, N and α will depend on the bulk plasma parameters in a way that is difficult to estimate without solving the fluid equations.

A second characteristic feature of anode spot onset is hysteresis in the electrode current–voltage characteristic. This hysteresis, shown in figure 6 and in several previous references [8, 21, 23, 35], can be understood qualitatively using the same concept that there be a critical number of ions in a Debye cube. The difference between the downswing in the voltage, i.e. decreasing the electrode bias in a spot mode, and the upswing in the voltage, i.e. increasing the electrode bias for initial onset of a spot from a glow, is that for the upswing the relevant Debye cube is located in the anode glow, while for the downswing it is located in the anode spot. As figure 9 depicts, when considering a Debye cube in the anode spot, ions are present not only from ionization within the cube, but also from the outflow of ions generated in the anode glow between the spot and the electrode. On the downswing, the anode spot remains as long as the number of ions, produced from the sum of these two sources, in each Debye cube in the anode spot exceeds the critical number. An obvious minimum electrode bias required to maintain the spot mode is that which makes $\Delta\phi_2 = 0$ in figure 9, which means that the total sheath energy is the ionization energy of the neutrals. Consistent with this assertion, our experiments have observed the spot to vanish before this limit is reached on the downswing of the electrode bias.

6. Anode spot equilibrium

In this section we consider two features of anode spot equilibrium: size and shape. The characteristic size of the anode spot, meaning the length of the quasineutral region between the anode glow and the double layer at the plasma/spot interface, can be estimated with a similar one-dimensional model as used in section 5. We assume that the ionization rate throughout the spot is approximately uniform. The flux of ions leaving the spot and entering the bulk plasma is equal to the rate of generation within the spot: $\Gamma_{i,as} = \Gamma_{e,b} n_n \sigma L$. From Bohm's criterion [40], ions leave at the ion sound speed in the spot, so this flux can also be written $\Gamma_{i,as} = n_{i,as} c_{s,as}$. Putting these together yields an estimate for the one-dimensional length of

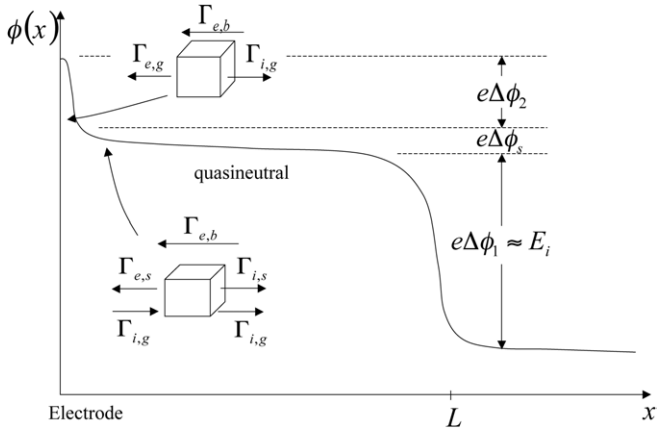

Figure 9. Schematic drawing showing the flux of ions and electrons entering and leaving Debye cubes in different regions of the anode spot.

the anode spot

$$L = \frac{n_{\mathrm{i,as}} c_{\mathrm{s,as}}}{\Gamma_{\mathrm{e,b}}} \frac{1}{n_{\mathrm{n}}\sigma}. \tag{7}$$

From the assumption of uniform generation of ions in the anode spot, Bohm's condition requires $\Delta\phi_{\mathrm{s}} \geqslant T_{\mathrm{e,as}}/e$. Since the 'average' ion is born in the middle of the anode spot rather than at a source on the high potential side, as is the case in a conventional presheath, the minimum potential drop is twice the conventional $T_{\mathrm{e}}/2e$. Assuming that the anode spot is only weakly collisional, we take $\Delta\phi_{\mathrm{s}} \approx T_{\mathrm{e,as}}/e$, so $c_{\mathrm{s,as}} \approx \sqrt{e\Delta\phi_{\mathrm{s}}/M_{\mathrm{i}}}$. The electron flux due to the beam is $\Gamma_{\mathrm{e,b}} = n_{\mathrm{e,b}}\sqrt{2e\Delta\phi_{\mathrm{l}}/m_{\mathrm{e}}}$, where $n_{\mathrm{e,b}}$ is the density in the spot. The density of electrons generated in the anode spot is much smaller than the density of electrons streaming into the spot from the bulk plasma, $n_{\mathrm{e,as}} \ll n_{\mathrm{e,b}}$, since $n_{\mathrm{i,as}} \approx n_{\mathrm{e,as}}\sqrt{M_{\mathrm{i}}/m_{\mathrm{e}}}$ and the anode spot is quasineutral. This is analogous to the results in section 5. So, $n_{\mathrm{e,b}} \gg n_{\mathrm{e,as}}$, which implies that $n_{\mathrm{e,b}} \approx n_{\mathrm{i,as}}$, and equation (7) can be written

$$L = \frac{1}{n_{\mathrm{n}}\sigma}\sqrt{\frac{m_{\mathrm{e}}}{M_{\mathrm{i}}}}\sqrt{\frac{\Delta\phi_{\mathrm{s}}}{2\Delta\phi_{\mathrm{l}}}}. \tag{8}$$

To estimate the length of the anode spots shown in figure 1 requires σ for the beam electrons streaming through the anode spot. This energy is derived from the energy gained by acceleration through the double layer, which is typically the ionization energy of the neutral gas ($E_{\mathrm{i}} \approx 17$ eV for argon [41]). From [41] we find that for 17 eV electrons that $\sigma \approx 1.7\times10^{-18}$ cm^2, but this value is sensitive to the particular energy near threshold. Assuming that the electron temperature in the anode spot is approximately the same as it is in the bulk plasmas implies $\Delta\phi_{\mathrm{s}} \approx T_{\mathrm{e}}$.

The fireball shown in figure 1(*b*) near a 10 mm diameter electrode was taken with a neutral pressure of 4 mTorr and the electron temperature was measured to be $T_{\mathrm{e}} \approx 1$ eV. The firerod shown in figure 1(*d*) near a 55 mm diameter electrode was with a neutral pressure of 1.5 mTorr and an electron temperature of $T_{\mathrm{e}} \approx 2$ eV. From the above estimates for σ and $\Delta\phi_{\mathrm{s}}$, equation (8) predicts that $L \approx 2.8$ cm for figure 1(*b*) and $L \approx 11$ cm for figure 1(*d*). From the photographs, these values are empirically found to be $L \approx 3$ cm and $L \approx 8$ cm respectively. Both estimates are within the accuracy of our estimate for the electron-impact ionization cross section σ which is sensitive to the precise electron energy.

The firerod shown in figure 1(*d*) has a curved shape that cannot be explained with this model. A possible explanation is that stray magnetic fields or Earth's magnetic field are responsible. It was observed that moving a weak permanent magnet outside the plasma chamber, which produced a field <2 G at the firerod location, was sufficient to straighten or otherwise change the curvature of the firerod. Regardless of the curvature, the radius and length of the firerod were essentially unchanged.

Equation (8) also predicts that $L \propto 1/P$. The $1/P$ scaling of the anode spot length has been observed in previous experiments, see e.g. [8] which also presents a similar model for the diameter of fireballs. Additional experiments testing equation (8) were carried out for anode spots observed near the aperture of the nonambipolar electron source [42]. These experiments, reported in [43], support equation (8) to within a few percent in a situation where an axial magnetic field was present.

We next consider the shape of the anode spot. Our experimental observations have shown that the anode spot is a fireball for small electrodes, but a firerod for larger electrodes, as shown in figure 1. Previous observations have typically reported fireballs, but firerods have also been reported in magnetized plasmas [16–18, 33], and recently also in an unmagnetized plasma near a spherical electrode [13].

When an anode spot forms, it significantly increases the effective electrode area for collecting the electrons diffusing to it from the bulk plasma. As described in section 4 and [2], if this effective area is too big to support a monotonically decreasing potential, either a double sheath must form or the plasma potential must be larger than the electrode potential, i.e. an ion sheath exist, to reduce the electron current reaching the electrode. This effect is a result of globally balancing the electron and ion currents lost from the plasma. Obviously if an ion sheath is present, an anode spot cannot be because there is no electron acceleration mechanism to increase the frequency of ionization and generate a spot. However, double sheaths can accompany anode spots when the effective electrode area exceeds a critical level. This leads to cylindrically shaped anode spots accompanied by global nonambipolar flow for large electrodes.

To understand why anode spots are cylindrically shaped for large electrodes, consider the global current balance of section 4 and equation (1). As described in section 4, the electrode surface area must satisfy $A_{\mathrm{E}}/A_{\mathrm{w}} < \mu$ for anode glow and spot formation. When a spot forms A_{E} effectively becomes the surface area of spot itself since all electrons in the bulk plasma that diffuse through this surface are lost to the electrode. If this typically much larger effective area does not satisfy $A_{\mathrm{E}}/A_{\mathrm{w}} < \mu$, the electrode collects too much electron current; i.e. electrons are lost to the electrode at a faster rate than ions are lost to other plasma boundaries. This current is reduced and a balance is established by the formation of a dip, or double sheath, where a monotonic electron sheath

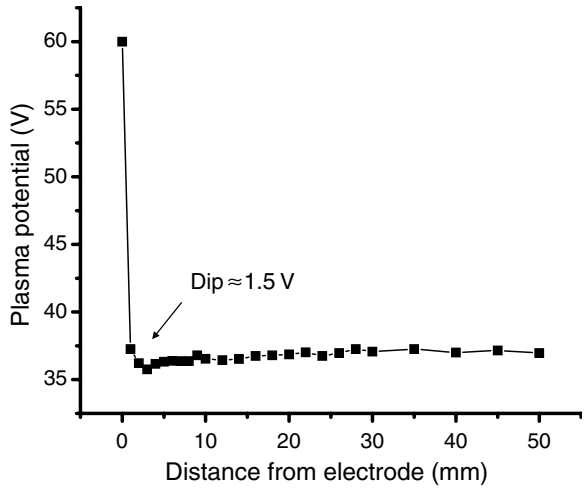

Figure 10. A double sheath potential profile (i.e. potential dip) measured with an emissive probe near an electrode biased at 60 V, which was supporting a firerod, but at a location away from the firerod.

would otherwise be. From the one-dimensional model and equation (8), the length of the spot is determined. Double sheaths, which retard electron current, form on parts of the electrode surface and, due to the reduced electron beam current, the spot is absent from these locations. This effectively shrinks the radial direction of the anode spot and forms a cylinder. The double sheath reduces the total electron current lost to the electrode by reducing its effective electron collecting area.

Experimentally, a contour plot of measured potentials should reveal the presence of double sheaths. Attempts at these measurements failed, however, because the holder of the electrostatic probe provided a sink for ions and electrons that significantly altered the anode spot in its vicinity. In particular, when firerods were present, the spot would move, or jump, to different locations on the electrode to avoid the probe. This suggests that there is no preferred location for the spot to form on the electrode, which is consistent with our model, but it eliminated the possibility of measuring the potential contour of a firerod with electrostatic probes. The only direct measurements that were achieved were for locations on the electrode away from the spot, e.g. that shown in figure 10, which confirms that double sheaths accompanied firerods at electrode locations away from the spot. The neutral pressure was 1.5 mTorr in this case and the dip depth was approximately 1.5 V which corresponds to the electron temperature (the energy needed to reflect most of the incident electrons).

When a firerod and accompanying double sheath were present, global nonambipolar flow was established in the plasma. This means that all electron loss was to the electrode while all ion loss was to the grounded chamber wall. This scenario was established by the bounding electric fields because the double layer at the electrode reflected all ions born in the bulk plasma and the plasma potential was large enough that all electrons were reflected from ion sheaths at the grounded chamber walls. A characteristic feature of this regime was that the difference between the electrode and plasma potential always 'locked' to a fixed value. The plasma potential and ion sheath at the chamber wall could thus be made, essentially, arbitrarily large. When this scenario was established in previous experiments by using an electrode with surface area satisfying, $\mu < A_E/A_w < [(0.6/\mu) - 1]^{-1}$, the plasma potential 'locked' to just a few volts less than the electrode potential. When anode spots were present, the 'locking' potential was a few volts less than the electrode potential minus the ionization potential of the neutral gas as shown in figure 7. This is because $e\Delta\phi_1 \approx E_i$ was required to sustain the spot.

A second characteristic feature of global nonambipolar flow was an electron temperature significantly hotter than the ambipolar value [2]. This was due to an increase in the confinement of high energy electrons and a decrease in the confinement of low energy electrons compared to the ambipolar case. In ambipolar flow, only electrons with an energy greater than that necessary to traverse the ion sheath at the chamber wall were lost. Electrons with less energy were confined. In global nonambipolar flow, all electrons incident on the electrode were lost, regardless of their energy. No electrons were lost to the chamber wall. Since the same electron current was lost in both cases, the electron energy confinement was enhanced in global nonambipolar flow. This effect is described in detail in [2]. Figure 8 shows measurements of this characteristic temperature increase when firerods, and the corresponding global nonambipolar flow, were present. In this case the ambipolar temperature was 0.8 eV while the global nonambipolar value was approximately 2.4 eV. Data shown in figures 7 and 8 were taken with the 55 mm diameter electrode at 1.5 mTorr neutral pressure.

The presence of global nonambipolar flow has implications for multiple concentric anode spots. Multiple concentric anode spots are stair step potential profiles, of height E_i/e and length L, that have a spherical shape and can form near small electrodes biased positive enough [23]. If the electrode is so big that the onset of one anode spot increases the electron collecting area of the electrode to a level that $A_E/A_w > \mu$, global nonambipolar flow ensues. As a consequence, the plasma potential 'locks' with the electrode. Multiple anode spots cannot then be generated because $\Delta\phi_2$ becomes fixed and no additional ionization can occur in the anode glow region. A natural prediction, then, is that one cannot generate multiple concentric *firerods* in an unmagnetized plasma.

If, however, the electrode is small enough that even with the effective increase in anode area due to a first anode spot, the condition $A_E/A_w < \mu$ is satisfied, potential 'locking' does not occur, and a second anode spot may form. The onset of the second spot may be analyzed in an analogous way as the first spot, predicting the condition that $\Delta\phi_2 \approx \Delta\phi_c$ for onset. Previous measurements [23] show concentric fireballs, so, presumably, the chamber and electrode satisfied $A_E/A_w < \mu$ with both spots present in these measurements. Our considerations do not exclude the possibility that an equilibrium state could be established where a firerod surrounds a fireball. However, to the best of our knowledge, such a state has yet to be observed.

One last feature of anode spot equilibrium we wish to briefly discuss is why the double layer potential drop is approximately the ionization potential of the neutral gas. This

relationship has been observed for argon here and in [8], for xenon in [43, 44], and additionally for hydrogen and neon in [13]. From the discussion in section 5 and above we have found that spots form due to increased ionization in the anode glow so, as long as $T_e \ll E_i$, the minimum double layer potential drop is apparently the threshold ionization potential of the neutral gas $e\Delta\phi_l \geqslant E_i$. However, the question remains: why is the potential drop typically equal to this minimum? Larger potential drops would not necessarily violate the global current balance, and an anode spot potential larger than the electrode potential could even be a solution in theory. The only solution that minimizes the input power to the plasma, however, requires that the double layer potential drop be equal to the ionization potential of the neutral gas.

The power source controlling the electrode inputs a power of $P_E = eI_eV_E$ in which I_e is the electron current reaching the electrode and V_E is electrode potential referenced to ground. The power input by the hot filaments is a constant equal to $P_f = eI_fV_f$. If the double layer potential drop were bigger than the minimum ionization potential, the electron current to the electrode I_e would increase by a corresponding amount due to increased ionization inside the anode spot. Assuming that the power input to the plasma is minimized implies that the double layer potential drop of an anode spot should be equal to the ionization potential of the neutral gas; in agreement with the experiments.

7. Conclusions

A diverse set of anodic double layer equilibrium states were found experimentally including double sheaths, anode glow and two types of anode spots: spherical fireballs and cylindrical firerods. Simple models based on the principle of current balance were constructed to determine which state was present for given experimental conditions. For $A_E/A_w > [(0.6/\mu) - 1]^{-1}$, the electrode sheath was an ion sheath, and no anodic double layer formed. For $\mu < A_E/A_w < [(0.6/\mu) - 1]^{-1}$, a double sheath existed, which is a type of anodic double layer. For $A_E/A_w < \mu$ anode glow and anode spot double layers were observed.

Anode glow formation was due to increased ionization in an electron sheath. A model was constructed which suggests that anode spots form from the anode glow when the number of ions in a Debye cube adjacent to the electrode balances the number of electrons in that same Debye cube. When this condition was met, a quasineutral plasma (anode spot) formed from the anode glow. Our model predicted that the critical electrode bias for the onset of an anode spot has an inverse neutral pressure scaling, which was confirmed experimentally. It also predicted hysteresis in the current–voltage characteristic of the electrode, which was also confirmed by experiment.

When an anode spot formed, it significantly increased the effective area of the electrode for collecting electrons. If the electrode and anode spot were small, the effective area could still satisfy $A_E/A_w < \mu$ and the potential monotonically decreased from the electrode to the plasma. In this case spherical fireballs were found. However, it often happened that the spot increased the effective electrode area beyond this value, and a combination of a double sheath and a cylindrical firerod formed. Double sheaths were directly measured using electrostatic probes at locations on the electrode surface where the firerod was absent. The presence of the double sheaths, necessary to preserve global current balance, at these locations caused the cylindrical shape of the firerod in an unmagnetized plasma. In this case, the effective electrode area satisfied $\mu < A_E/A_w < [(0.6/\mu) - 1]^{-1}$ and global nonambipolar flow was present. Global nonambipolar flow implies that all electrons are lost to the electrode while all positive ions are lost to the chamber wall. Two characteristic features of global nonambipolar flow; potential 'locking' and electron temperature enhancement, were confirmed with experiment. A one dimensional model for the anode spot size was developed, which agreed with our experimental measurements as well as with previous measurements [43]. The model also predicted an inverse neutral pressure dependence of the spot size that was observed in previous works [8].

Acknowledgments

This material is based upon work supported under a National Science Foundation Graduate Research Fellowship (S.D.B.) and by U.S. D.O.E. Grant No DE-FG02-97ER54437.

References

[1] Langmuir I 1929 *Phys. Rev.* **33** 954
[2] Baalrud S D, Hershkowitz N and Longmier B 2007 *Phys. Plasmas* **14** 042109
[3] Nakamura Y, Nomura Y and Stenzel R L 1981 *J. Appl. Phys.* **52** 1197
[4] Matsubara A, Tonegawa A, Shibuya T, Sato K, Kawamura K and Takayama K 2001 *J. Appl. Phys.* **89** 5326
[5] Charles C 2007 *Plasma Sources Sci. Technol.* **16** R1
[6] Emeleus K G 1982 *Int. J. Electronics* **52** 407
[7] Conde L, Ferro Fontán C and Lambás J 2006 *Phys. Plasmas* **13** 113504
[8] Song B, D'Angelo N and Merlino R L 1991 *J. Phys. D: Appl. Phys.* **24** 1789
[9] Song B, D'Angelo N and Merlino R L 1992 *J. Phys. D: Appl. Phys.* **25** 938
[10] Sanduloviciu M, Borcia C and Leu G 1995 *Phys. Lett.* A **208** 136
[11] Strat M, Strat G and Gurlui S 1999 *J. Phys. D: Appl. Phys.* **32** 34
[12] Gurlui S, Agop M, Strat M, Strat G and Băcăiţă S 2005 *Japan. J. Appl. Phys.* **44** 3253
[13] Stenzel R L, Ionita C and Schrittwieser R 2008 *Plasma Sources Sci. Technol.* **17** 035006
[14] Oprescu B and Popescu S 2000 *J. Phys. D: Appl. Phys.* **33** 2284
[15] Tang D and Chu P K 2003 *J. Appl. Phys.* **94** 1390
[16] An T, Merlino R L and D'Angelo N 1994 *J. Phys. D: Appl. Phys.* **27** 1906
[17] Barkan A and Merlino R L 1995 *Phys. Plasmas* **2** 3261
[18] Mihai-Plugaru M, Ivan L M and Dimitriu D G 2006 *J. Optoelectron. Adv. Mater.* **7** 845
[19] Conde L and León L 1999 *IEEE Trans. Plasma Sci.* **27** 80
[20] Ivan L M, Amarandei G, Aflori M, Mihai-Plugaru M, Gaman C, Dimitriu D G and Sanduloviciu M 2005 *IEEE Trans. Plasma Sci.* **33** 544

[21] Ivan L M, Amarandei G, Aflori M, Mihai-Plugaru M, Dimitriu D G, Ionita C and Schrittwieser R W 2005 *Acta Phys. Slovaca* **55** 501
[22] Aflori M, Amarandei G, Ivan L M, Dimitriu D G and Sanduloviciu M 2005 *IEEE Trans. Plasma Sci.* **33** 542
[23] Dimitriu D G, Aflori M, Ivan L M, Ionita C and Schrittwieser R W 2007 *Plasma Phys. Control Fusion* **49** 237
[24] Lozneanu E, Popescu S and Sanduloviciu M 2002 *IEEE Trans. Plasma Sci.* **30** 32
[25] Conde L and León L 1994 *Phys. Plasmas* **1** 2441
[26] Nerushev O A, Novopashin S A, Radchenko V V and Sukhinin G I 1998 *Phys. Rev.* E **58** 4897
[27] Druyvesteyn M J and Penning F M 1940 *Rev. Mod. Phys.* **12** 87
[28] Rubens S M and Henderson J E 1940 *Phys. Rev.* **58** 446
[29] Sanduloviciu M and Lozneanu E 1986 *Plasma Phys. Control Fusion* **28** 585
[30] Seyhoonzadeh A, Forsling P, Bailey M, Rosario R, Beardsley K, Tao J and Lonngren K E 1988 *Phys. Fluids* **31** 682
[31] Ahedo E 1996 *Phys. Plasmas* **3** 3875
[32] Song B, Merlino R L and D'Angelo N 1992 *Phys. Scr.* **45** 395
[33] Song B, Merlino R L and D'Angelo N 1992 *IEEE Trans. Plasma Sci.* **20** 476
[34] Torvén S and Anderson D 1979 *J. Phys. D: Appl. Phys.* **12** 717
[35] Chiriac S, Dimitriu D G and Sanduloviciu M 2007 *Phys. Plasmas* **14** 072309
[36] Song B, Merlino R L and D'Angelo N 1992 *Phys. Scr.* **45** 391
[37] Conde L 2004 *Phys. Plasmas* **11** 1955
[38] Lapuerta V and Ahedo E 2000 *Phys. Plasmas* **7** 2693
[39] Limpaecher R and MacKenzie K R 1973 *Rev. Sci. Instrum.* **44** 726
[40] Bohm D 1949 *Characteristics of Electrical Discharges in Magnetic Fields* ed A Guthrie and R K Wakerling (New York: McGraw-Hill) chapter 3
[41] Straub H C, Renault P, Lindsay B G, Smith K A and Stebbings R F 1995 *Phys. Rev.* A **52** 1115
[42] Longmier B, Baalrud S and Hershkowitz N 2006 *Rev. Sci. Instrum.* **77** 113504
[43] Longmier B 2007 Plasma sheath behavior in a total nonambipolar radio frequency generated plasma electron source *PhD Thesis University of Wisconsin, Madison* pp 104–26
[44] Longmier B and Hershkowitz N 2008 *Rev. Sci. Instrum.* **79** 093506